Natural Resources, 2026, 17(11), 335-366
https://www.scirp.org/journal/nr
ISSN Online: 2158-7086
ISSN Print: 2158-706X

Hydrochemical Charcterization and Suitability for Irrigation of Groundwater in the Lékoumou (Southwest of the Republic of Congo)

Gilbert Bassakouahou[1*], Hartman Issombo Elenga[1], Djohn Josia Weaver Mboussa[1], Lydie Natacha Mpika Ngouaka[2], Urbain Gampio Mbilou[2], Medard Ngouala Mabonzo[3]

[1]Georesources and Exploration Laboratory, School of Mines, Hydraulics and Energy, Denis Sassou Nguesso University, Brazzaville, Republic of the Congo
[2]Geosciences and Environment Laboratory, Department of Geology, Faculty of Science and Technology, Marien Ngouabi University, Brazzaville, Republic of the Congo
[3]Geographic Institute, Faculty of Letters, Arts and Human Sciences, Marien Ngouabi University, Brazzaville, Republic of the Congo
Email: *bassakouahougilbrt@gmail.com

How to cite this paper: Bassakouahou, G., Elenga, H.I., Mboussa, D.J.W., Ngouaka, L.N.M., Mbilou, U.G. and Mabonzo, M.N. (2026) Hydrochemical Charcterization and Suitability for Irrigation of Groundwater in the Lékoumou (Southwest of the Republic of Congo). *Natural Resources*, **17**, 335-366.
https://doi.org/10.4236/nr.2026.1711018

Received: September 2, 2026
Accepted: October 8, 2026
Published: November 19, 2026

Copyright © 2026 by author(s) and Scientific Research Publishing Inc.
This work is licensed under the Creative Commons Attribution International License (CC BY 4.0).
http://creativecommons.org/licenses/by/4.0/
Open Access

Abstract

This study was carried out following a water drilling campaign intended for drinking water supply in the Lékoumou department. Its objective was to assess the suitability of the groundwater for consumption and irrigation. Ten (10) water samples were collected from ten (10) boreholes. The physical parameters, namely temperature (T), pH, TDS and electrical conductivity (EC), were measured *in situ*, whereas the physicochemical analyses carried out at the laboratory of La Congolese des Eaux (LCDE) covered turbidity, total hardness (TH), the major cations and anions, and some trace metal elements. The results indicate that, overall, the physicochemical parameters of the groundwater studied fall within the acceptability thresholds and guideline values recommended by the World Health Organization (WHO) for drinking water. Its chemical composition is mainly dominated by the HCO_3^-, Ca^{2+} and Mg^{2+} ions, with a clear dominance of the calcium-magnesium bicarbonate hydrochemical facies. The analysis of the bivariate diagrams and of the Gibbs diagram highlights water-rock interaction as the main process controlling the mineralization of the groundwater of the Lékoumou. Regarding its suitability for irrigation, the application of the Wilcox criteria indicates that the water studied falls, overall, into the excellent to good categories. However, the suitability of this water for human consumption cannot be guaranteed on the basis of physicochemical parameters alone. Regular and rigorous monitoring of the microbiological parameters remains necessary to confirm its potability. Thus,

the implementation of an appropriate policy for monitoring the physicochemical and microbiological quality of the water would be an essential means of durably guaranteeing its potability and contributing to the preservation of the health of the population.

Keywords

Groundwater, Hydrochemistry, Physicochemical Parameters, Water Quality, Lékoumou Aquifer

1. Introduction

Water is a beverage essential to life [1] [2]. Access to safe drinking water is a fundamental human right promoted by international organizations [3] [4], because water is the main constituent of living organisms [5] [6].

In the Republic of the Congo, access to drinking water remains a major problem in several urban and rural centers [7]. Paradoxically, the Congo has substantial water resources, notably surface water and groundwater [8]. However, only 66% of the population in urban areas and 47% in rural areas have access to drinking water [9]. A significant share of the population, namely 3.3%, obtains its water from hand-dug wells, 2.3% from rainwater and watercourses, and 17% from unimproved sources [10].

In rural areas, the lack of adequate water distribution and treatment services considerably exposes the population to waterborne diseases owing to the direct consumption of surface water.

The population of the Lékoumou department, for example, faces a lack of water distribution and treatment services. This situation forces the population to turn to surface water sources to meet their domestic, agricultural and pastoral needs. To improve access to drinking water in rural areas, several projects have been implemented, notably through groundwater abstraction and the establishment of water supply points. In this context, several boreholes have been drilled in the Lékoumou department to tap the groundwater. Groundwater is often considered to be a better-quality resource for drinking water supply because of its relative protection against direct contamination. However, this water resides in geological formations (aquifers), and its physicochemical composition is strongly influenced by hydrogeological conditions, water-rock interactions and anthropogenic activities [11].

In the Lékoumou department, scientific knowledge about the chemical and physicochemical quality of the groundwater of the whole aquifer remains limited and very fragmentary. Nevertheless, the few available data, such as those obtained by [12] reveal a low mineralization of the water in certain localities, but these limited data do not allow the geochemical processes or mechanisms controlling the mineralization of this water, nor its suitability for agricultural use, to be characterized in a general, let alone exhaustive, manner. This lack of data constitutes a scientific obstacle, limiting the implementation of water management and water

security mechanisms.

In this context, an in-depth assessment of the hydrochemical quality of the groundwater is essential to guarantee the potability of the water and to better understand the mineralization processes. This approach makes it possible to properly identify the natural and anthropogenic factors influencing water quality, thus contributing to good management of water resources.

The objective of the present study is to assess the physicochemical quality of the groundwater of the Lékoumou department, to identify the geochemical processes responsible for the mineralization of this water, to assess its suitability for human consumption with respect to international drinking water quality standards, and finally to assess its suitability for agricultural use.

2. Materials and Methods

2.1. Study Area

The Lékoumou department is located in the southwest of the Republic of the Congo, between 0˚52'00" south latitude and 14˚49'00" east longitude, and covers an area of 20,950 km^2 (**Figure 1**).

The area has a humid tropical climate [13] of the AW4 type according to the Köppen classification [14]. This climate is characterized by intertropical low pressures from October to May, and by the austral subtropical high pressures and

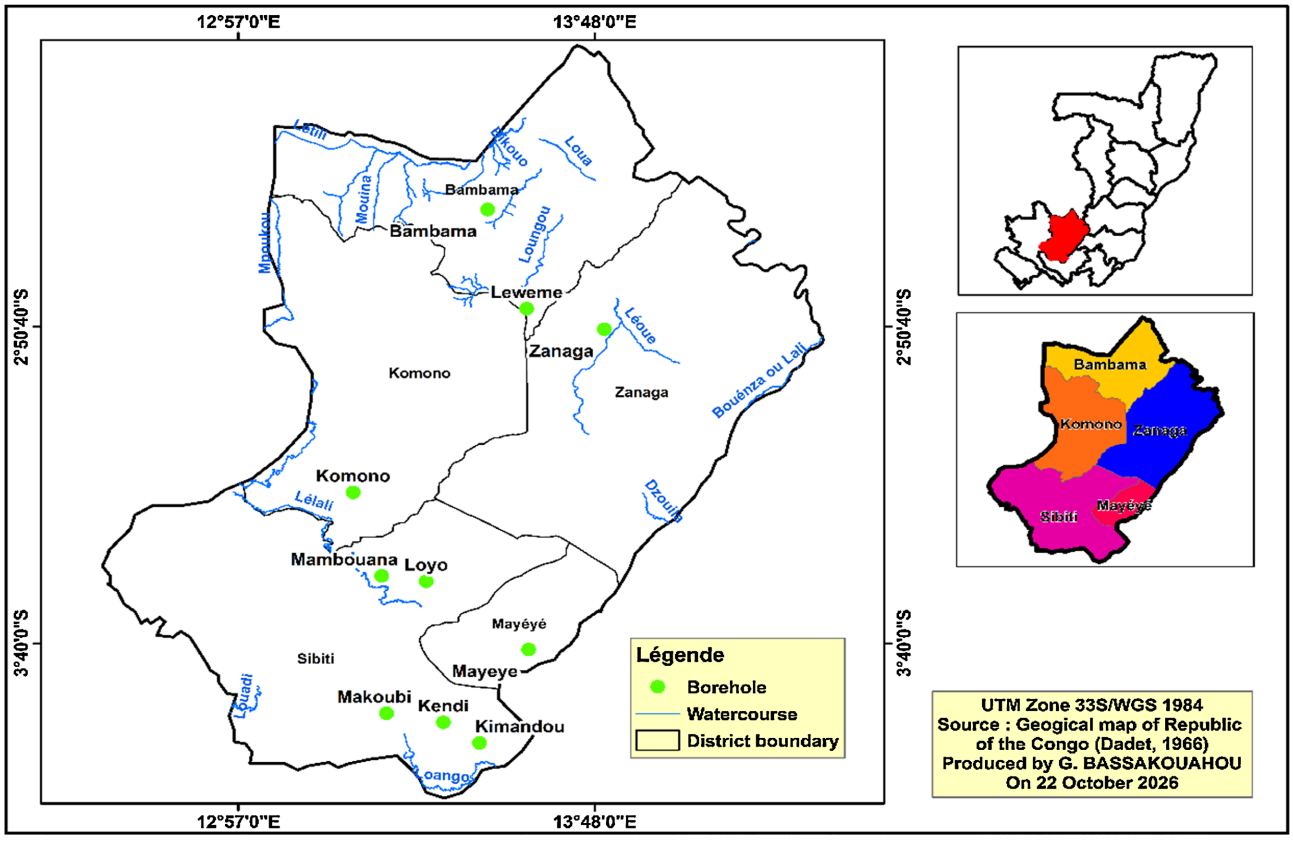


Figure 1. Location of the study area and sampled points (boreholes).

the cold waters of the Benguela current from June to September. Mean annual temperatures range between 20˚C and 27˚C. Mean precipitation varies between 1400 and 2000 mm. This tropical climate regime shows a sharp contrast between a long rainy season from October to May and a dry season, without rain, from June to September.

The soils of the area fall into three major classes, namely: strongly desaturated and reworked ferralitic soils developing on sandy, slightly clayey materials; hydromorphic soils developing on alluvial or colluvial materials; and finally, podzolic soils, which are sandy and acidic [15]-[17]. The vegetation growing on these soils is dominated by forest, covering 84% of the territory, against 16% of savanna [18].

From a geological standpoint, according to the authors [19]-[21], the Lékoumou department is dominated in the east by a granitic basement, with the presence of metamorphic enclaves (quartzites, amphibolites) and basic to ultrabasic intrusions on the one hand, and in the west by sedimentary formations (sandstone, limestone and clay) on the other. These formations favor the exploitation of a shallow aquifer through boreholes and wells (**Figure 2**).

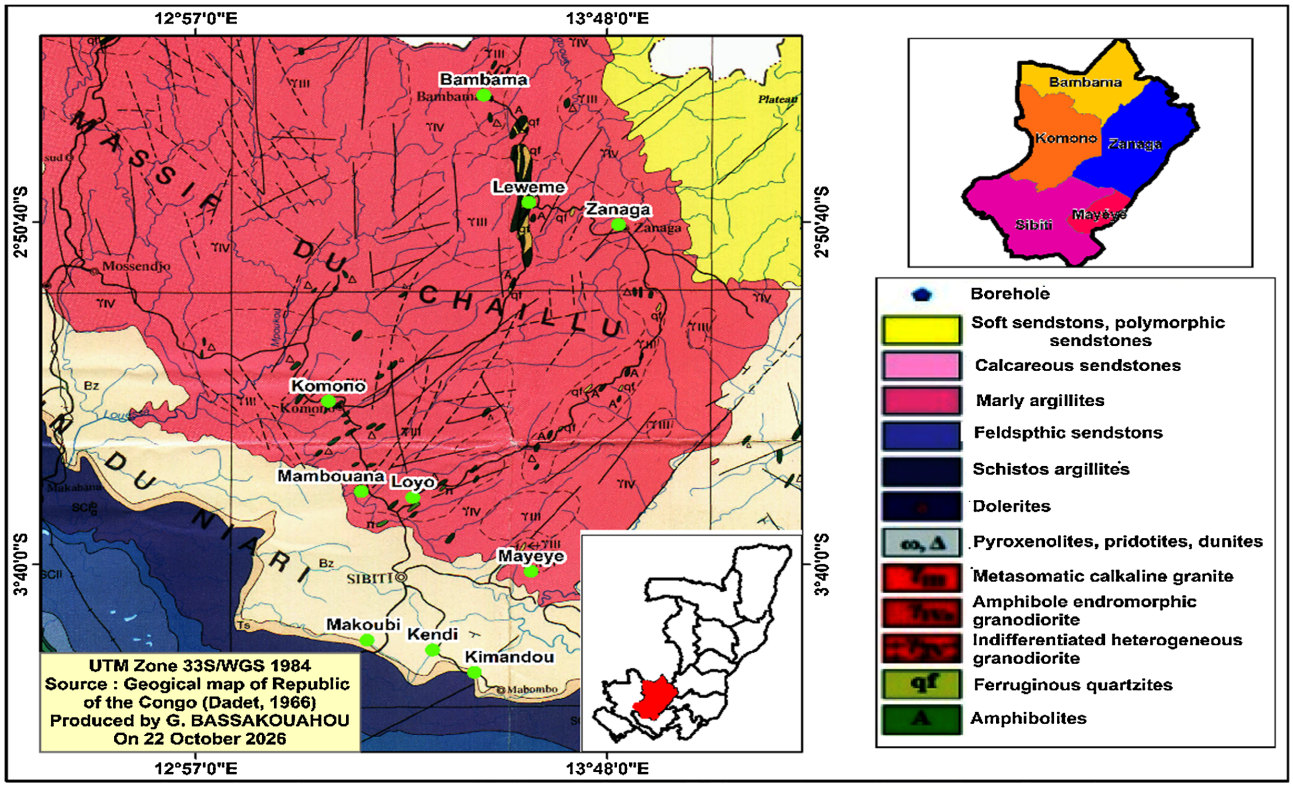


Figure 2. Geological map of the study area and boreholes.

2.2. Water Sampling and Analysis

Water samples were collected during a drilling campaign carried out in December 2025 (wet season). The ten boreholes were selected according to the geological context of the study area (**Figure 1**). After collection, the samples were stored in 1 L polyethylene bottles, kept at 4˚C in a cooler fitted with ice packs, and trans-

ported to the laboratory of La Congolaise des Eaux (LCDE) for analysis.

The coordinates of the sampled boreholes (Table 1) were recorded using a Garmin GPSMAP 64sx receiver. The boreholes are distributed as follows:

- Granitic basement of Chaillu: seven (7) boreholes (Loyo, Mamb, Kom, Lewé, Zan, Bam and May);
- Sedimentary formations of the Bouenza subgroup: three (3) boreholes (Mak, Ken and Kim).

The two main geological contexts of the study area are thus represented: the granitic basement (seven boreholes) and the sedimentary formations of the Bouenza subgroup (three boreholes).

As sampling was carried out during a single campaign, seasonal variability could not be assessed; repeated sampling in both the wet and dry seasons is recommended. The conclusions therefore apply only to the boreholes sampled in the study area and should not be extrapolated to the entire region.

Table 1. Geographic coordinates and depths of the boreholes.

Borehole	Longitude X	Latitude Y	Altitude	Depth
Mak	03˚51'43.4"	013˚17'153"	368	57 m
Loyo	03˚30'26.8"	013˚22'45.5"	464	28
Mamb	03˚29'46.7"	013˚19 '09.7"	464	28
May	03˚41'069"	013˚38'21.6"	408	43
Ken	03˚52'186"	013˚26'129"	354	36
Kam	03˚55'15.1"	013˚31'36.2"	361	42
Kom	03˚16'29.1"	013˚13'17.4"	461	47
Zan	02˚50'52.5"	013˚49'18.8"	578	52
Lewe	02˚47'532"	013˚38'051"	605	46
Bamb	02˚32'28.8"	013˚32'27"	586	54

2.3. Physicochemical Analyses of the Water

The physicochemical parameters, namely temperature (T˚), pH, electrical conductivity (EC) and TDS, were measured in the field using a WWT 82362 multiparameter meter, and turbidity (Turb) was determined using a HACH 2100N turbidimeter. The chemical parameters, namely Ca^{2+}, Mg^{2+}, Na^{+}, K^{+}, NO_3^-, HCO_3^-, SO_4^{2-}, Cl^-, SiO_2, F^-, TH, and the trace elements Fe^{2+}, Mn^{2+}, Cu^{2+}, Zn^{2+}, were analyzed in the laboratory. The elements Ca^{2+}, Mg^{2+}, HCO_3^- and Cl^- were determined by titrimetry using a Digital UACH 2800 titrator; the ions K^+, Na^+, NO_3^- and SO_4^{2-} were determined by ion chromatography. The metals were determined using an atomic absorption spectrometer (detection limit 0.001 mg/L). The results of the physicochemical parameter analyses are compared with the [22] [23] (Table 2) in order to assess the potability of the water of the aquifer studied.

2.4. Assessment of the Quality of the Analyses

The quality of the analyses was assessed using the ionic balnce method (ε). This method makes it possible to assess the reliability of the measurements carried out [24], in order to accept or reject the results of the chemical analyses.

The ionic balance is calculated using the following formula:

$$\mathcal{E} = \frac{\sum \text{Cations} - \sum \text{Anions}}{\sum \text{Cations} + \sum \text{Anions}} \times 100$$

As a general rule, the analysis results are assessed according to the following classification:

- $-1\% < \mathcal{E} < +1\%$ Excellent analysis results
- $-5\% < \mathcal{E} < +5\%$ Acceptable reliability of the analysis results
- $-10\% < \mathcal{E} < +10\%$ Mediocre reliability of the analysis results
- $\mathcal{E} < -10\%$ or $\mathcal{E} > +10\%$ Poor reliability of the analysis results

Beyond 10%, or below −10%, of the ionic balance, the analysis results are considered poor [25].

The results of all the analyses of our samples show an ionic balance of less than 5% (ionic balance between −1 and 0). The analysis results are therefore judged excellent for processing.

2.5. Hydrochemical Facies of the Data

The hydrochemical facies are determined using the Piper diagram software. This diagram consists of two triangles, which represent the cationic and anionic chemical facies, and a diamond synthesizing the overall facies of all the water samples analyzed [26].

2.6. Statistical Analysis of the Data

Statistical analyses were performed with XLSTAT (version 2016) on 10 samples and 18 physicochemical variables. Pairwise relationships between variables were assessed using the Pearson correlation coefficient [27].

Iron (Fe), copper (Cu) and manganese (Mn) were below the limit of detection (LOD) in most samples. These non-detected values were replaced by LOD/2 in order to retain the whole dataset. Because the variables concerned are almost constant, their correlations and their positions in the multivariate analyses partly reflect this substitution rather than genuine geochemical variability. These three elements were therefore kept in the calculations but were not used to interpret geochemical processes: the interpretation relies on the parameters quantitatively measured in all samples.

A principal component analysis (PCA) was applied to the Pearson correlation matrix, which amounts to centering and scaling the variables. It was used to project the variables onto the factorial axes in order to identify the dominant geochemical processes controlling mineralization. No rotation was applied. Axes were retained according to a minimum cumulative variance threshold of 70%: F1

(65.80%) and F2 (14.40%) together explain 80.20% of the total variance. The results are presented as a correlation circle and a distance biplot.

An agglomerative hierarchical clustering (AHC) was applied to the variables (column clustering), using Euclidean distance and Ward's aggregation method. The variables were neither centered nor scaled for the AHC: the clusters therefore partly reflect the magnitude of the values, which limits their interpretation. They were interpreted jointly with the PCA results, which were obtained on standardized variables. The number of clusters was determined by XLSTAT's automatic truncation (entropy criterion).

Given the small sample size (n = 10), the large number of variables (p = 18) and the presence of substituted non-detected values, these multivariate analyses are exploratory in nature. The factorial axes and the clusters are interpreted as trends and working hypotheses, without significance testing, and will need to be confirmed on a larger dataset.

2.7. Gibbs Diagram

The Gibbs diagram method, developed by Gibbs, was applied to strengthen the understanding of the natural geochemical mechanism controlling the mineralization of all the groundwater in the study area. This approach makes it possible to distinguish three main mechanisms likely to influence the chemical composition of the water [28]: input from precipitation (meteoric dominance), water-rock interaction (lithogenic dominance) or concentration by evaporation (evaporitic dominance). This diagram requires the calculation of two ionic ratios, namely:

$$\text{Gibbs ratio}(1) = \frac{Na^+}{Na^+ + Ca^{2+}}$$

$$\text{Gibbs ratio}(2) = \frac{Cl^-}{Cl^- + HCO_3^-}$$

These results thus make it possible to explain the spatial and temporal variations in groundwater quality and to highlight the area's most likely to be affected by water-rock dissolution processes or by increased salinization. This method is reinforced by bivariate diagrams for a good understanding of the mechanism.

The values of the chemical and physicochemical parameters were compared with the guideline values of the World Health Organization [22] for drinking water [29].

2.8. Suitability of the Water for Irrigation

The assessment of water quality and suitability for irrigation is an indispensable operation for good crop productivity and quality as well as for soil fertility. Water suited to irrigation promotes crop growth and soil fertility [30]. The suitability of groundwater for irrigation is assessed by determining indicators such as: the sodium percentage (%Na), the magnesium adsorption ratio (MAR), the sodium adsorption ratio (SAR) and the permeability index (PI). These indices are calculated

respectively using the following equations:

$$SAR = \frac{Na^+}{\sqrt{\left(Ca^{2+} + Mg^{2+}\right)/2}}$$

$$\%Na = \frac{Na^+}{Ca^{2+} + Mg^{2+} + Na^+ + K^+} \times 100$$

$$MAR = \frac{Mg^{2+}}{Ca^{2+} + Mg^{2+}} \times 100$$

$$PI = \frac{Na^+ + \sqrt{HCO_3^-}}{Ca^{2+} + Mg^{2+} + Na^+} \times 100$$

By combining these calculations with the Wilcox and USSL diagrams of the Piper diagram software, a good appraisal of the quality of the water for irrigation is obtained. These diagrams involve another indicator, electrical conductivity. Electrical conductivity (EC) makes it possible to assess the degree of mineralization and the salinity risk of irrigation water.

3. Results

3.1. Physicochemical Parameters

In situ, the physicochemical parameters measured were temperature (T˚), electrical conductivity (EC), total dissolved solids (TDS) and hydrogen potential (pH).

Figures 3(a)-(e) and **Table 2** present the results of the *in situ* physicochemical parameters. All pH values fall within the WHO acceptability range (6.5 - 8.5) [23], and TDS values do not exceed 600 mg/L, the threshold corresponding to good palatability [23]. The WHO sets no guideline value for temperature or electrical conductibility; these two parameters are therefore discussed without reference to a WHO threshold.

Temperature is a physical parameter that plays an important role in modifying chemical and physical properties as well as biological reactions [31]. Across all the sampled points, the measured temperature values show small variations. The values range between 23˚C and 25˚C, with a mean of 24˚C and a standard deviation of 0.32˚C. The temperatures of the water studied do not exceed the [23] standard (22˚C - 25˚C).

Electrical conductivity (EC), which designates the ability of water to conduct electric current [32] [33], depends mainly on the concentration, nature, charge and mobility of the dissolved ions, as well as on the water temperature [34]. The conductivity measured in the aquifer water shows considerable variations between the different points. Values range from 19 to 310 µS/cm, with a mean of 155 µS/cm and a standard deviation of 111.07 µS/cm. The highest EC values were measured at three points located in the sedimentary formations, namely Mak (310 µS/cm), Kim (306 µS/cm) and Ken (209 µS/cm). The WHO does not set a guideline value for EC [23]. Since all TDS values are below 600 mg/L, the WHO acceptability

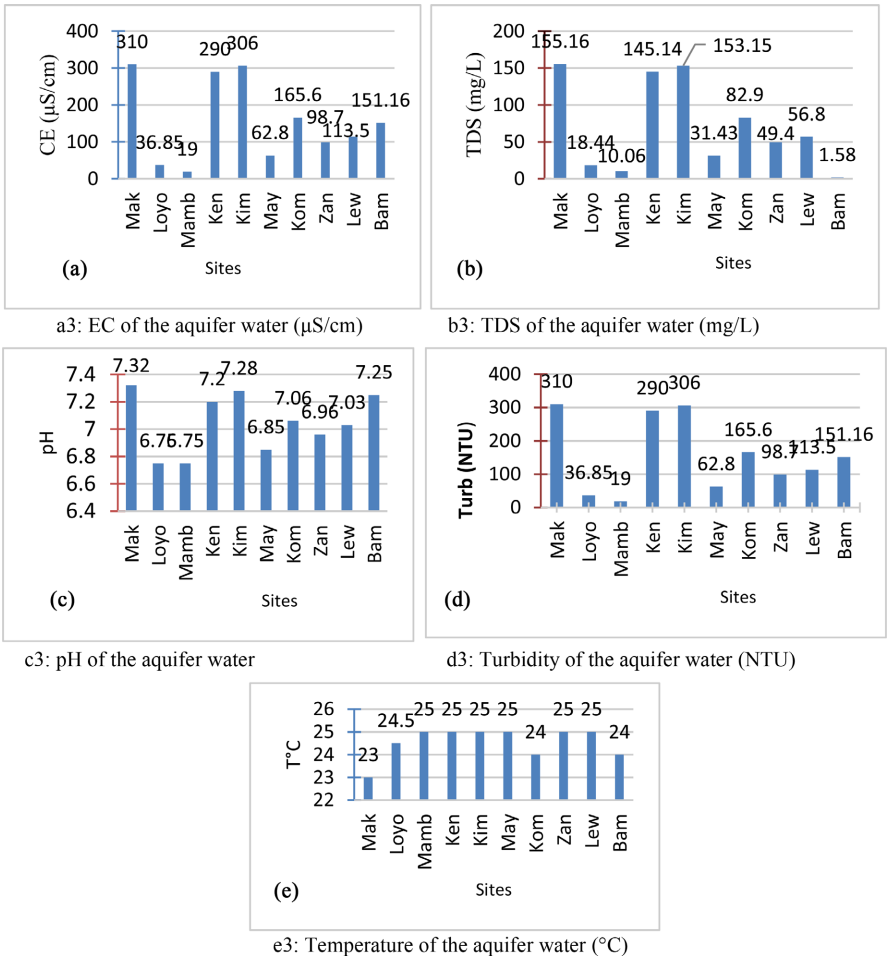


Figure 3. *In situ* physicochemical parameters.

criterion for palatability, the measured EC values are consistent with wearkly mineralized water.

The hydrogen potential (pH) is a physicochemical parameter that characterizes the acid-base state of an aqueous solution. pH plays a decisive role in the dissolution and precipitation reactions of minerals [35]. The pH measured at all the sampled points shows a tendency towards neutrality. The values vary very slightly between 6.75 and 7.32, with a mean of 7.04 and a standard deviation of 0.22. All the pH recorded fall within the WHO acceptability range (6.5 - 8.5) [23].

Total dissolved solids (TDS) represent the sum of the constituents dissolved in water, in ionic form, but also certain molecular species and dissolved organic substances [36]. All the TDS values are below 600 mg/L, the WHO acceptability criterion for good palatability [23], but they vary strongly from one sampling point to another. The lowest value was measured at Bam (1.58 mg/L) and the highest at Mak (155.16 mg/L), with a mean of 70.41 mg/L and a standard deviation of 60.55 mg/L.

Turbidity expresses the cloudy appearance of water. High turbidity can reduce the effectiveness of disinfection and may be associated with a health risk. In the

study area, turbidity values at all the sampled points are below the WHO acceptability values of 5 NTU [23]. Value ranges from 1.06 to 2.05 NTU, with a mean of 1.55 NTU and a standard deviation of 0.29 NTU. However, all values exceed the value of 1 NTU recommended by the WHO for effective disinfection, so the water would need appropriate treatment before being used for drinking.

In the laboratory, the physicochemical parameters analyzed are the major ions (Ca^{2+}, Na^{+}, SO_4^{2-}, HCO_3^{-}, Cl^{-}, F^{-}, NO_3^{-}, K^{+}, Mg^{2+}), other elements, notably silica (SiO_2), hardness and some trace metal elements, Fe^{2+}, Mn, Pb^{2+}, Cu^{2+}, Zn^{2+} and Al^{3+}.

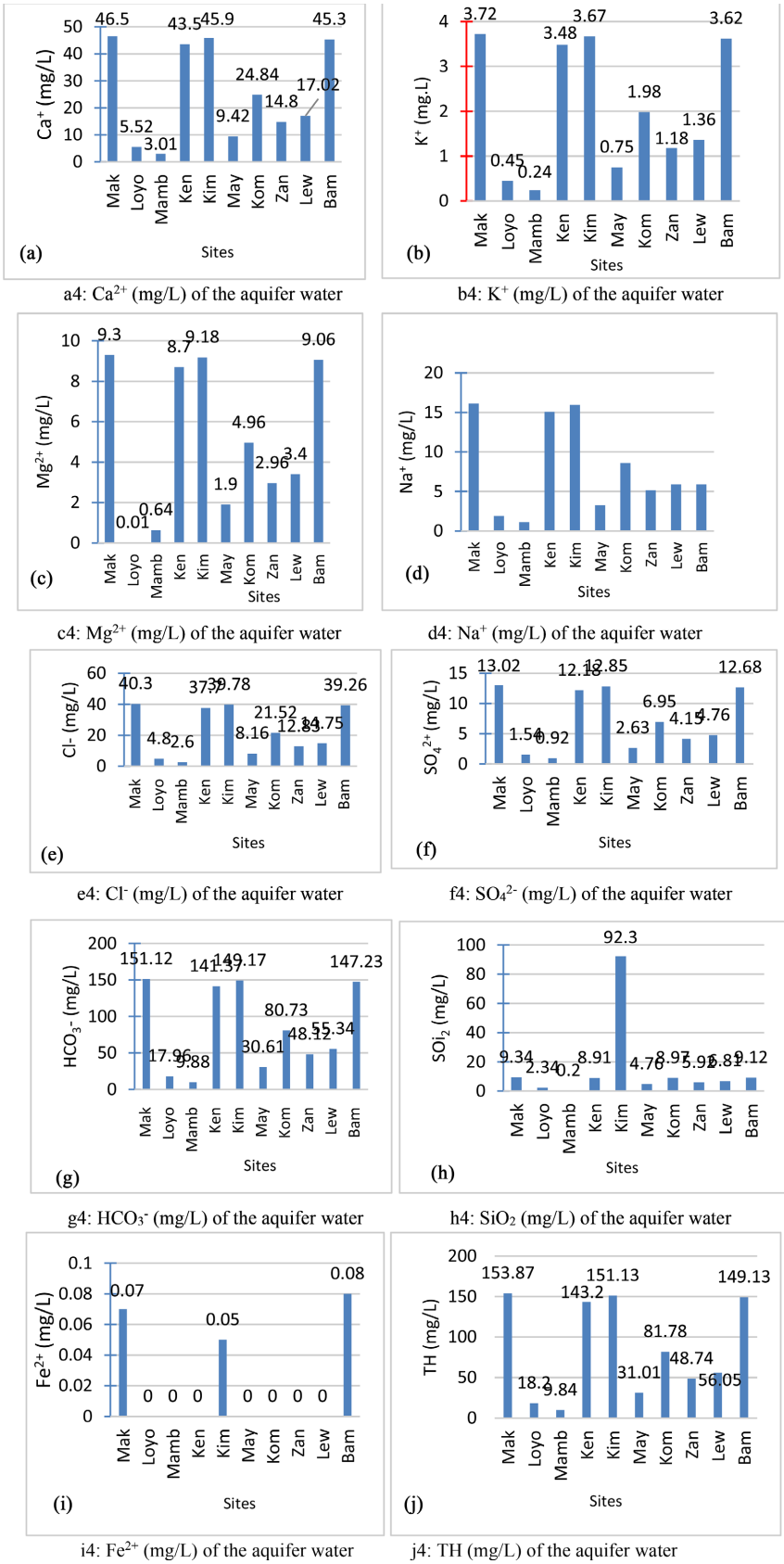
The results in **Figures 4(a)-(j)** and **Table 2** concerning the major ions show variations from one sampling point to another. The WHO does not set health-based guideline values for these major ions [23], so their concentrations are described here withour a compliance assessment. Across all the sampled points, Ca^{2+} concentrations range from 3.01 mg/L (Mamb) to 46.50 mg/L (Kim), with a mean of 25.58 mg/L and a standard deviation of 18.02 mg/L. Na^{+} ranges from 1.12 mg/L (Mamb) to 16.12 mg/L (Mak), with a mean of 7.90 mg/L and standard deviation of 5.81 mg/L. K^{+} ranges from 0.24 mg/L (Mamb) to 3.72 mg/L(Mak), with a mean of 2.05 mg/L and a standard deviation of 1.44 mg/L. SO_4^{2-} concentrations also vary between points, from 0.92 mg/L (Mak) to 13.02 mg/L (Kim), with a mean of 7.17 mg/L and a standard deviation of 5.04 mg/L. Mg^{2+} ranges from 0.01 mg/L (Loyo) to 9.30 mg/L (Mak), with a mean of 4.08 mg/L and a standard deviation of 3.88 mg/L. HCO_3^{-} varies considerably between points, from 9.88 mg/L (Mamb) to 151.12 mg/L (Mak), with a mean of 83.15 mg/L and a standard deviation of 58.56 mg/L.

The other parameters, namely silica, total hardness (TH) and the trace elements, show a different pattern. Silica ranges from 0.20 mg/L (Mamb) to 92.30 mg/L (Kim), with a mean of 14.86 mg/L and a standard deviation of 27.38 mg/L. Total hardness of the aquifer water ranges from 9.84 to 153.87 mg/L (as $CaCO_3$), with a mean of 84.30 mg/L and a standard deviation of 59.44 mg/L. The WHO sets no health-base guideline value for hardness [23]. According to the usual hardness classification (<60 mg/L soft; 60 - 120 mg/L moderately hard; 120 - 180 mg/L hard), the aquifer water ranges from soft to hard, with most points in the soft to moderately hard classes.

Trace elements are for the most part absent (below the detection limit), with the exception of the Fe, which was detected at four points (Mak, Kim, Lew and Bam) at low concentrations of 0.07, 0.05, 0.02 and 0.08 mg/L, respectively. The WHO sets no health-base guideline value for iron; concentrations above about 0.3 mg/L may cause staining and affect the taste and appearance of water. All detected values are below this level. Fluoride (F-) was not detected at any of sampled points.

3.2. Hadrochemical Facies of the Groundwater

The facies of the groundwater of the area are obtained from two diagrams, Piper and Schoeller-Berkaloff.



a4: Ca^{2+} (mg/L) of the aquifer water

b4: K^{+} (mg/L) of the aquifer water

c4: Mg^{2+} (mg/L) of the aquifer water

d4: Na^{+} (mg/L) of the aquifer water

e4: Cl^{-} (mg/L) of the aquifer water

f4: SO_4^{2-} (mg/L) of the aquifer water

g4: HCO_3^{-} (mg/L) of the aquifer water

h4: SiO_2 (mg/L) of the aquifer water

i4: Fe^{2+} (mg/L) of the aquifer water

j4: TH (mg/L) of the aquifer water

Figure 4. Concentrations of the different parameters of the aquifer water.

Table 2. Descriptive statistics of the results.

Variable	Minimum	Maximum	Mean	Std. deviation
pH	6.750	7.320	7.045	0.215
T°C	23.000	25.000	22.500	0.000
Turbidity	1.060	2.050	1.556	0.285
TDS	1.580	155.160	70.406	60.549
EC (µS/cm)	19.000	310.000	155.361	111.068
NH_4^+ (mg/l)	0.000	0.001	0.000	0.000
Cu^{2+} (mg/l)	0.000	0.001	0.000	0.000
Mn^{2+} (mg/L)	0.000	0.001	0.000	0.000
Ca^{2+} (mg/L)	3,01	46.500	25,581	18.02
Mg^{2+} (mg/L)	0.000	9.300	4.077	3.875
SO_4^{2-} (mg/L)	0.920	13.020	7.168	5.036
Cl^- (mg/L)	2.600	40.300	22.170	15.620
K^+ (mg/L)	0.240	3.720	2.045	1.441
Na^+ (mg/L)	1.120	16.120	7.898	5.807
Fe^{2+} (mg/L)	0.000	0.080	0.020	0.033
HCO_3^- (mg/L)	9.880	151.120	83.153	58.556
SiO_2 (mg/L)	0.200	92.300	14.867	27.384
T.H (mg/L)	9.840	153.870	84.295	59.442

1) Facies from the Piper diagram

The analysis of the water results on the Piper diagram shows a homogeneity of the chemical facies (**Figure 5**). The dominant facies highlighted in the groundwater is of the calcium-magnesium bicarbonate type. However, a singularity is observed at point Ken, which shows a depletion in magnesium and an enrichment in sodium and potassium. This point is characterized by a calcium-sodium-potassium bicarbonate facies. It is located in the southern part of the aquifer, which drains the sedimentary formations.

2) Chemical facies of the water according to the Schoeller-Berkaloff diagram

The Schoeller diagram (**Figure 6**) is a semi-logarithmic graphical representation [33]. In this diagram, the different ions are represented on the x-axis and the content of each ion is plotted on the y-axis. The points obtained are joined by straight line segments that make it possible to read the facies of the water sample concerned directly. The analysis of the diagram shows a perfect similarity in the shape of the line segments for all the water of the aquifer. One exception is made for a single point, which shows a different shape because of its low Mg^{2+} ion concentration. Overall, among the sampled water points, bicarbonate and calcium ions are predominant.

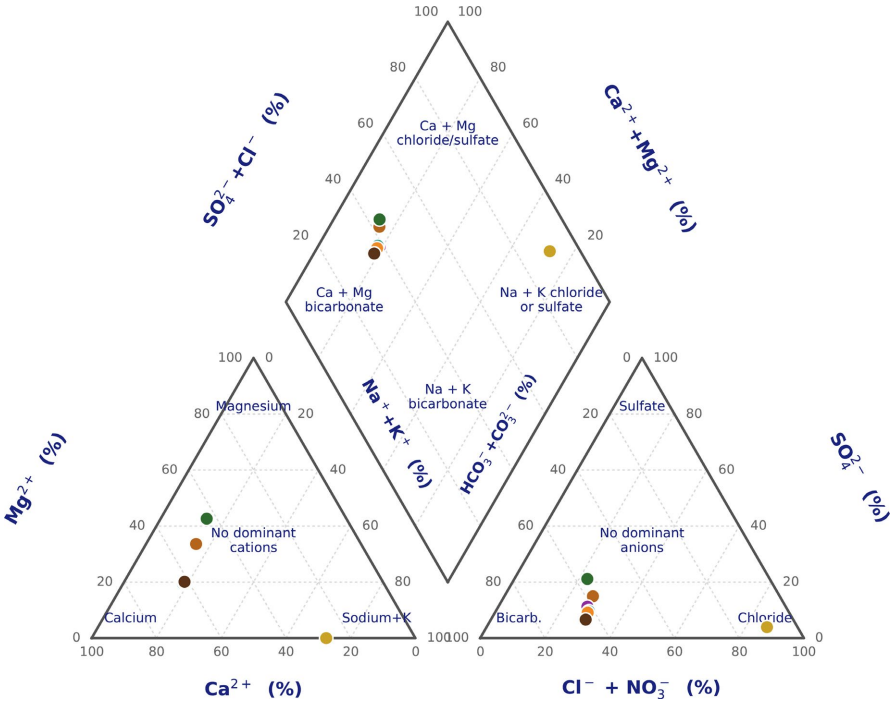


Figure 5. Piper diagram.

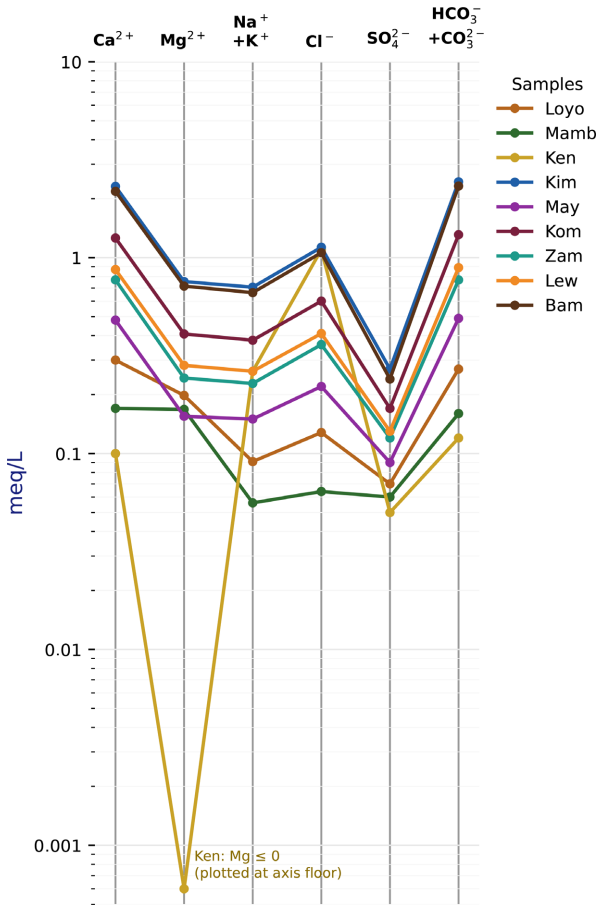


Figure 6. Schoeller-Berkaloff diagram.

3.3. Statistical Analysis

1) Pearson correlation analysis

Correlation analysis between variables makes it possible, using statistical tools such as the Pearson correlation coefficient, to monitor changes in water quality, to detect possible sources of pollution and to deepen the understanding of the dynamics of groundwater bodies, by examining how variations in one parameter are accompanied by those in another. The correlation is said to be positive when two parameters evolve in the same direction, that is, when they increase or decrease simultaneously [37].

Table 3 presents the Pearson correlation matrix of the aquifer water parameters. Correlations are described as very strong when the $r \geq 0.90$ and strong when $0.70 \leq r < 0.90$. The analysis of this table shows that pH is very correlated with TH (0.98), SO_4^{2-}, K^+ and HCO_3^- (0.92), and EC (0.91), and strongly correlated with Na^+ (0.87), and Ca^{2+} (0.76). The variables evolving together with very strong correlations are: Ca^{2+}-Mg^{2+} (0.99), Na^+-TDS (0.96) and EC-TDS (0.92). Na^+ and Cl- are strongly correlated (0.87). HCO_3^- ions show strong with Ca^{2+} (0.71), Mg^{2+} (0.76) and Na^+ (0.87).

2) Principal component analysis (PCA) and agglomerative hierarchical clustering (AHC)

The analysis of Figure 7 shows that 80.20% of the total information is retained

Table 3. Correlation matrix of the groundwater samples of the Lékoumou.

Variables	pH	Turb	TDS	EC	NH_4^+	Ca^{2+}	Mg^{2+}	SO_4^{2-}	Cl^-	K^+	Na^+	Fe^{2+}	HCO_3^-	SiO_2	T.H
pH	**1**														
Turb	0.11	**1**													
TDS	0.709	−0.20	**1**												
EC (µS/cm)	0.91	−0.20	0.922	**1**											
NH_4^+ (mg/l)	0.44	−0.24	0.492	0.489	**1**										
Ca^{2+} (mg/l)	0.76	−0.26	0.353	0.579	0.481	**1**									
Mg^{2+} (mg/l)	0.796	−0.22	0.380	0.606	0.474	0.996	**1**								
SO_4^{2-} (mg/l)	0.97	−0.17	0.69	0.918	0.408	0.716	0.738	**1**							
Cl^- (mg/l)	0.97	−0.18	0.693	0.918	0.408	0.716	0.738	0.500	**1**						
K^+ (mg/l)	0.977	−0.18	0.693	0.918	0.408	0.716	0.738	0.400	1.000	**1**					
Na^+ (mg/l)	0.872	−0.20	0.958	0.994	0.497	0.525	0.553	0.870	0.870	0.870	**1**				
Fe^{2+} (mg/l)	0.742	−0.27	0.254	0.546	0.532	0.899	0.886	0.759	0.758	0.758	0.474	**1**			
HCO_3^- (mg/l)	0.977	−0.17	0.693	0.918	0.408	0.716	0.738	0.340	0.400	0.500	0.770	0.758	**1**		
SiO_2 (mg/l)	0.47	−0.29	0.53	0.55	−0.07	0.530	0.529	0.485	0.485	0.485	0.562	0.372	0.485	**1**	
T.H (mg/l)	0.978	−0.18	0.694	0.918	0.411	0.717	0.739	0.478	0.400	0.500	0.871	0.759	0.700	0.484	**1**

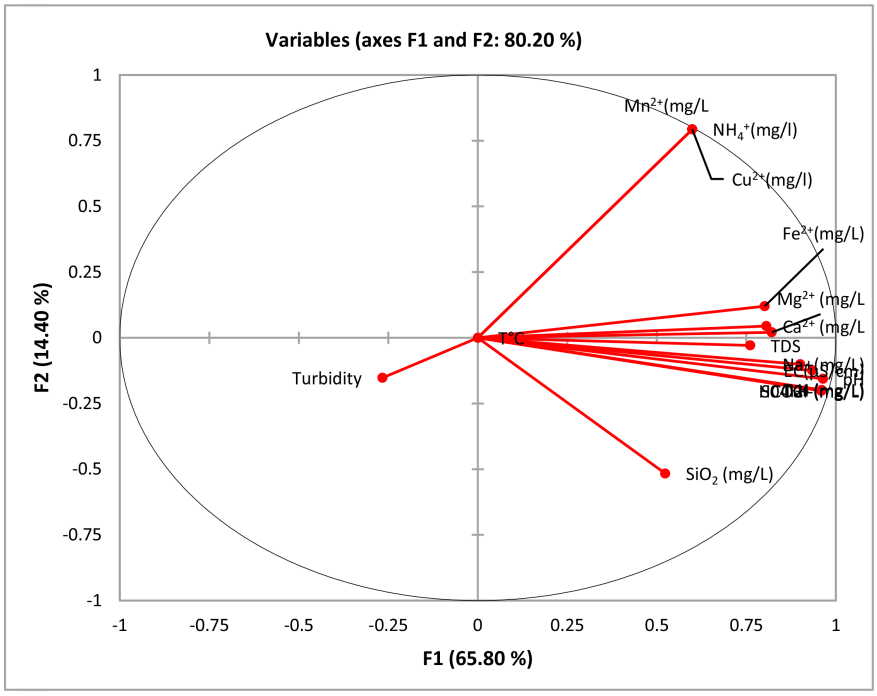


Figure 7. Factorial projection of the variables.

on the F1-F2 factorial plane, of which 65.80% is on axis F1 and 14.40% on axis F2. Axis F1 is strongly positively correlated with most of the variables: EC, TDS, Ca^{2+}, Mg^{2+}, Na^{+}, K^{+}, HCO_3^-, Cl^-, SO_4^{2-}, TH and Fe^{2+} (Table 4). Axis F2 is correlated only with trace metal elements, which are barely detected in the sampled water.

Combining the PCA results with those of the agglomerative hierarchical clustering (AHC), Figure 8(a), Figure 8(b), makes it possible to identify three groups. The first group is a plane represented by almost all the variables, notably Ca^{2+}, Mg^{2+}, Na^{+}, K^{+}, Cl^-, SO_4^{2-} and Fe^{2+}; this group represents the whole of the mineralization of the sampled water. The second and third groups are opposite to group 1. The second group is represented by three variables: TDS, HCO_3^- and TH. The third group is represented only by conductivity (EC), which illustrates the low mineralization of all the water of the aquifer.

3.4. Origin of the Mineralization of the Groundwater

1) Gibbs diagram

The Gibbs diagram (Figure 9) shows that almost all the water samples lie in the central domain, corresponding to the dominance of rock weathering. The ratios $Na^+/(Na^+ + Ca^{2+})$ and $Cl^-/(Cl^- + HCO_3^-)$ lie mainly between 0.2 and 0.3, while the TDS values vary from 15 to 600 mg/L. Only one sample stands out with a very low TDS value, between 1 and 2 mg/L, and thus falls in the precipitation dominance domain. No groundwater sample lies close to the evaporation dominance domain.

These results suggest that the mineralization of the groundwater of the study area is mainly controlled by water-rock interactions, notably by the dissolution

Table 4. Correlation between the variables and the factors.

	F1	F2
pH	**0.964**	−0.156
T °C	0.000	0.000
Turbidity	−0.266	−0.152
TDS	**0.761**	−0.029
EC (µS/cm)	**0.934**	−0.125
NH_4^+ (mg/L)	0.599	0.793
Cu^{2+} (mg/L)	0.599	0.793
Mn^{2+} (mg/L)	0.599	0.793
Ca^{2+} (mg/L)	**0.806**	0.044
Mg^{2+} (mg/L)	**0.821**	0.021
SO_4^{2-} (mg/L)	**0.960**	−0.202
Cl^- (mg/L)	**0.960**	−0.202
K^+ (mg/L)	**0.960**	−0.201
Na^+ (mg/L)	**0.901**	−0.101
Fe^{2+} (mg/L)	**0.801**	0.120
HCO_3^- (mg/L)	**0.960**	−0.202
SiO_2 (mg/L)	0.524	−0.517
T.H (mg/L)	**0.961**	−0.198

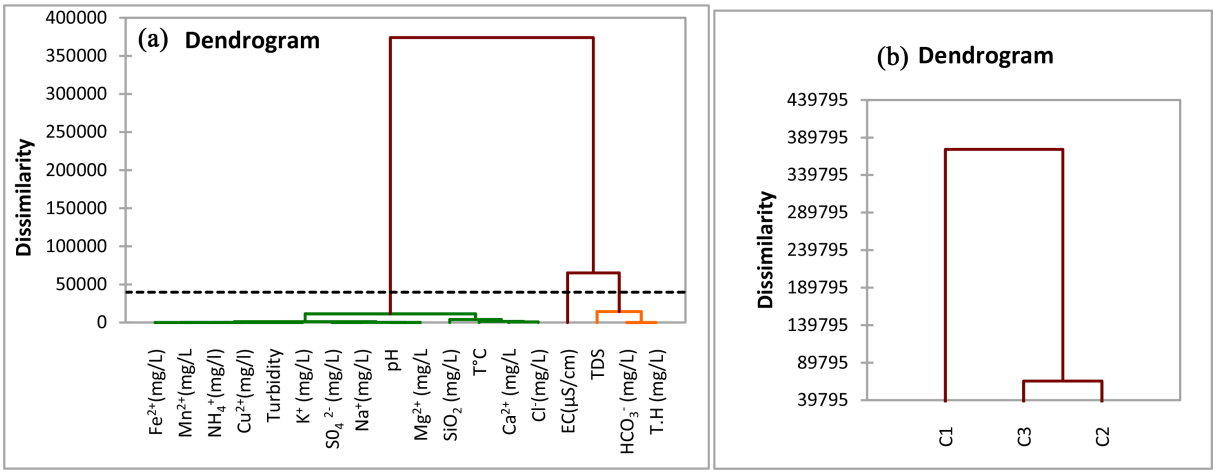


Figure 8. Dendrogram for the classification of the groundwater points.

of the minerals making up the bedrock. The small proportion of samples associated with the precipitation domain indicates, for its part, that the direct influence of meteoric inputs on the chemical composition of the water remains limited.

The plot of $(Ca^{2+} + Mg^{2+})$ vs HCO_3^- (**Figure 10(c)**) shows a strong correlation

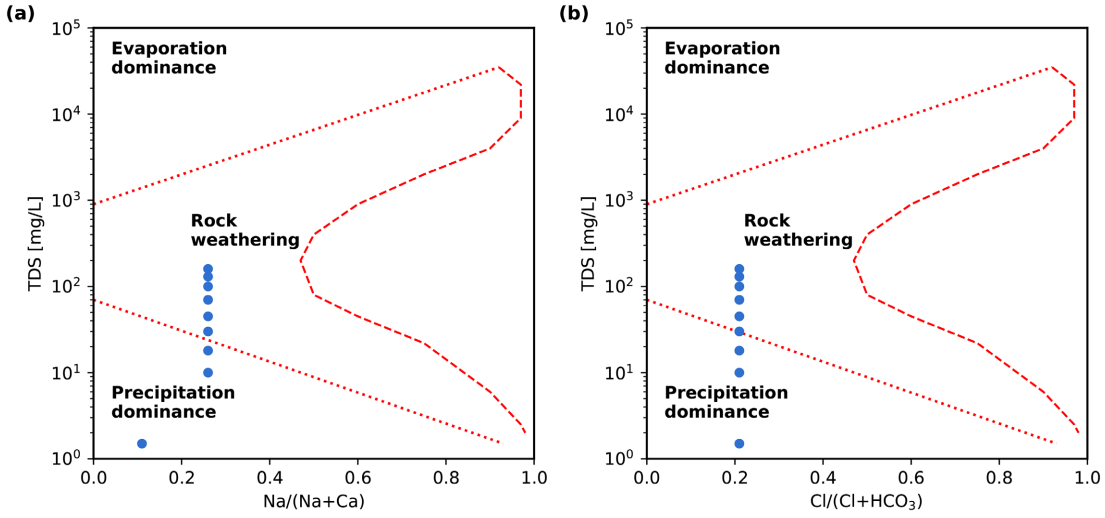


Figure 9. Gibbs diagram of the groundwater.

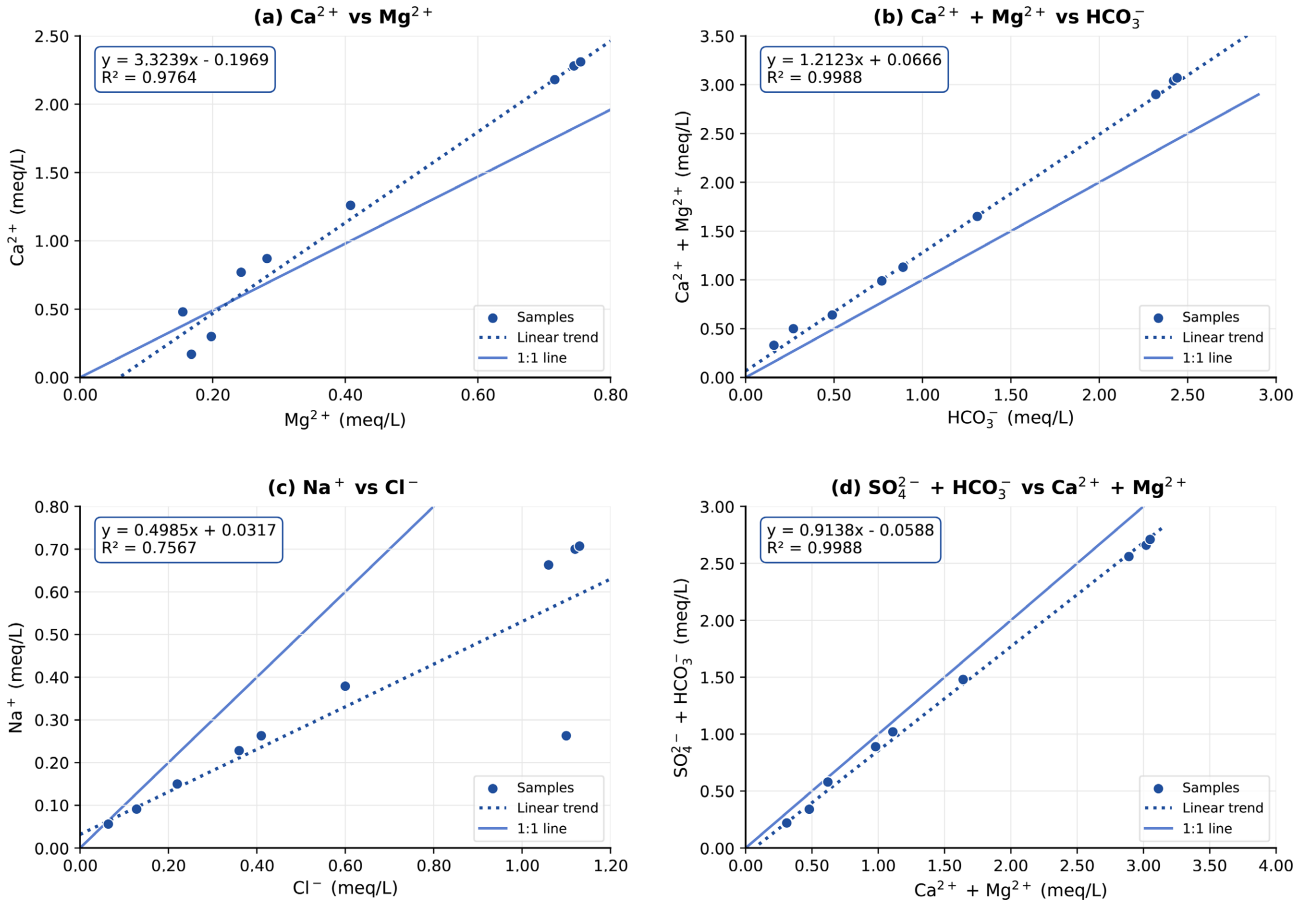


Figure 10. Bivariate diagrams between different chemical parameters.

($R^2 = 0.99$), with samples lying above the 1:1 line, which reflects an excess of $Ca^{2+} + Mg^{2+}$ ions over bicarbonate HCO_3^- ions.

2) Correlation Analysis of chemical Parameters

The bivariate plots (**Figure 10**) show the relationships between the chemical

parameters Ca^{2+} vs Mg^{2+} (Figure 10(a)), (SO_4^{2-} + HCO_3^-) vs (Ca^{2+} + Mg^{2+}) (Figure 10(d)), (Ca^{2+} + Mg^{2+}) vs HCO_3^- (Figure 10(b)) et Na^+ vs Cl^- (Figure 10(c)).

The Ca^{2+} vs Mg^{2+} plot (Figure 10(a)) shows a strong correlation between these two parameters (R^2= 0.97). On this plot, nearly all samples lie above the 1:1 line, indicating Ca^{2+} is greater than Mg^{2+}; only two samples lie below this line, with an excess of Mg^{2+}.

The (SO_4^{2-} + HCO_3^-) vs (Ca^{2+} + Mg^{2+}) plot (Figure 10(d)), a strong correlation is established (R2= 0,99) between these parameters. All samples lis below the 1:1 line, incating a clear predominance of (Ca^{2+} + Mg^{2+}) over (SO_4^{2-} + HCO_3^-).

The (Ca^{2+} + Mg^{2+}) vs HCO_3^- plot (Figure 10(b)) shows a strong correction (R^2 = 0.99), with samples lying above the 1:1 line, which reflects an excess of Ca^{2+} + Mg^{2+} ions over bicarbonate (HCO_3^-).

The Na^+ versus Cl^- diagram (Figure 10(c)) shows a strong positive correlation (Pearson's r = 0.87; R^2 = 0.76), with a regression slope of approximately 0.50. All samples plot below the 1:1 line, indicating a Cl^- excess and a Na^+ depletion in all samples. One sample (Cl^- ≈ 1.10 meq/L; Na^+ ≈ 0.26 meq/L) plots far below the 1:1 equivalent line and departs from the regression trend, showing the largest Na^+ deficit. Although the strong correlation suggests a common origin for Na^+ and Cl^-, the slope, which is markedly lower than 1, and the absence of any sample above the 1:1 line suggest that halite dissolution alone cannot explain their concentrations. The Na^+ depletion could result from reverse ion exchange (Na^+ adsorbed onto clays in exchange for Ca^{2+} and Mg^{2+}) or from an additional source of Cl^-, such as anthropogenic inputs.

3) Suitability of the water for irrigation

The assessment of the suitability of the groundwater for irrigation was made possible by calculating several hydrochemical indicators, notably the sodium percentage (%Na), the sodium adsorption ratio (SAR), the magnesium adsorption ratio (MAR) and the permeability index (PI). The use of the Wilcox and USSL diagrams made it possible to complete this assessment in order to appraise the risk associated with sodium and soil salinity.

a) Sodium percentage (%Na)

The sodium percentages calculated for all the groundwater samples (Table 5) range between 10.40% and 25.55%, with a mean of 20.07% and a standard deviation of 3.75%. The Wilcox [38] classification presents water with a sodium percentage (%Na) below 20% as excellent for irrigation, while water between 20 and 40% is considered good. Thus, all the water samples studied fall between the excellent and good categories.

b) Sodium adsorption ratio (SAR)

The sodium adsorption ratio (SAR) makes it possible to assess the risk of sodium accumulation in the soil. The SAR values of the samples studied vary from 0.15 to 0.56 (Table 5), with a mean of 0.35. According to the classification, water with a SAR below 10 is placed in class 1 (S1), that is, water with a low sodium hazard, whereas water with a SAR between 10 and 18, between 18 and 26, or even

above 26 is distributed among the medium, high and even very high hazard levels. All the water samples studied have a SAR below 10. Thus, all the water samples are in class S1, with a low sodium hazard.

c) Magnesium adsorption ratio

When water with high Mg^{2+} contents is used for agricultural purposes, it can lead to a degradation of soil structure, as well as an increase in its salinity [39]. High Mg^{2+} contents in groundwater favor exchanges with Na^{+}, which is likely to lead to soil alkalinization and a decrease in crop yield [40]. The magnesium adsorption ratio (MAR) of the water studied (**Table 5**) ranges between 18.50 and 25.96%, with a mean of 24.30% and a standard deviation of 2.07%. According to the classification proposed by [41], water with a MAR below 50% is considered favorable for irrigation, whereas above 50% the water is considered unsuitable, with negative effects on crops by making soils more saline [42]. All the water samples studied have a MAR below 50%. Thus, this water is classified in the category of water suitable for irrigation.

Table 5. Values of the indices for assessing the suitability of the water for irrigation.

Samples	Calculated			
	%Na	MAR	SAR	PI
1	20.50	24.81	0.56	42.26
2	25.55	18.50	0.22	151.43
3	21.26	25.96	0.15	160.01
4	20.53	24.81	0.55	43.63
5	20.43	24.80	0.56	43.21
6	20.50	24.96	0.25	92.35
7	20.49	24.78	0.41	57.26
8	20.51	24.82	0.32	73.91
9	20.51	24.78	0.41	68.99
10	10.40	24.81	0.21	47.87

d) Permeability index (PI)

Soil permeability is affected by prolonged use of irrigation water, depending on the soil type and the quality of the water used [42]. The permeability index makes it possible to assess the suitability of water for irrigation. The permeability indices calculated for all the aquifer samples (**Table 5**) vary from 160.01% to 42.26%, with a mean of 78.42% and a standard deviation of 43.44%. According to the [43] classification, 30% of the samples belong to class I (PI > 75%) and 70% to class II (25% ≤ PI ≤ 75%). Thus, 100% of the aquifer water samples are suitable for irrigation.

e) Classification according to the Wilcox diagram

Figure 11 shows the classification of the water according to the Wilcox diagram. This diagram makes it possible to assess the suitability of water for irrigation

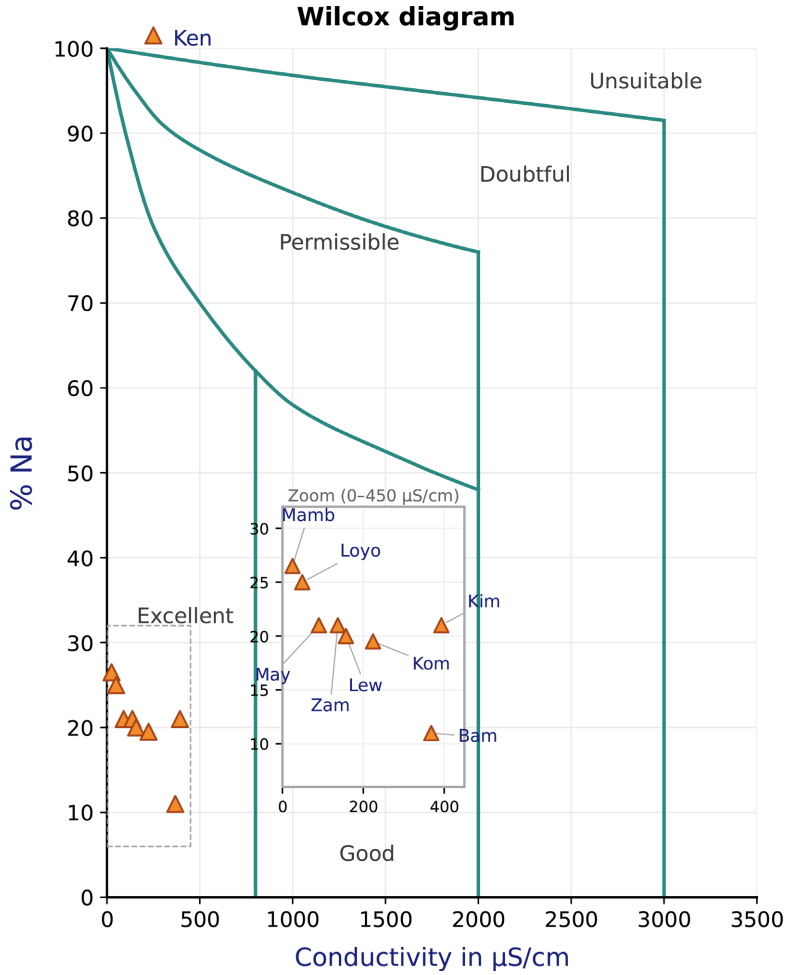


Figure 11. Wilcox diagram of the water.

from EC, plotted on the x-axis, and %Na, plotted on the y-axis. The water samples are distributed among different irrigation suitability classes ranging from excellent to poor. The analysis of all the samples shows that 90% of the samples fall in the excellent category and 10% belong to the good category.

f) Classification of the water according to the USSL diagram

Figure 12 presents the classes of the water studied according to the USSL diagram, taking EC and SAR into account. This diagram classifies the samples by combining the salinity hazard (C1-C4) and the sodicity hazard (S1-S4). The analysis of Figure 12 shows that 70% (7) of the water samples studied belong to class C1S1, characterized by low salinity and low sodicity, while 30% (3) of the samples are classified as C2S1, presenting a low salinity hazard and a medium sodicity hazard.

4. Discussion

1) Physicochemical characteristics and evolution of the mineralization of the water Parameters measured *in situ*

a) pH and temperature

The temperatures of the aquifer water are low, varying between 23˚C and 25˚C.

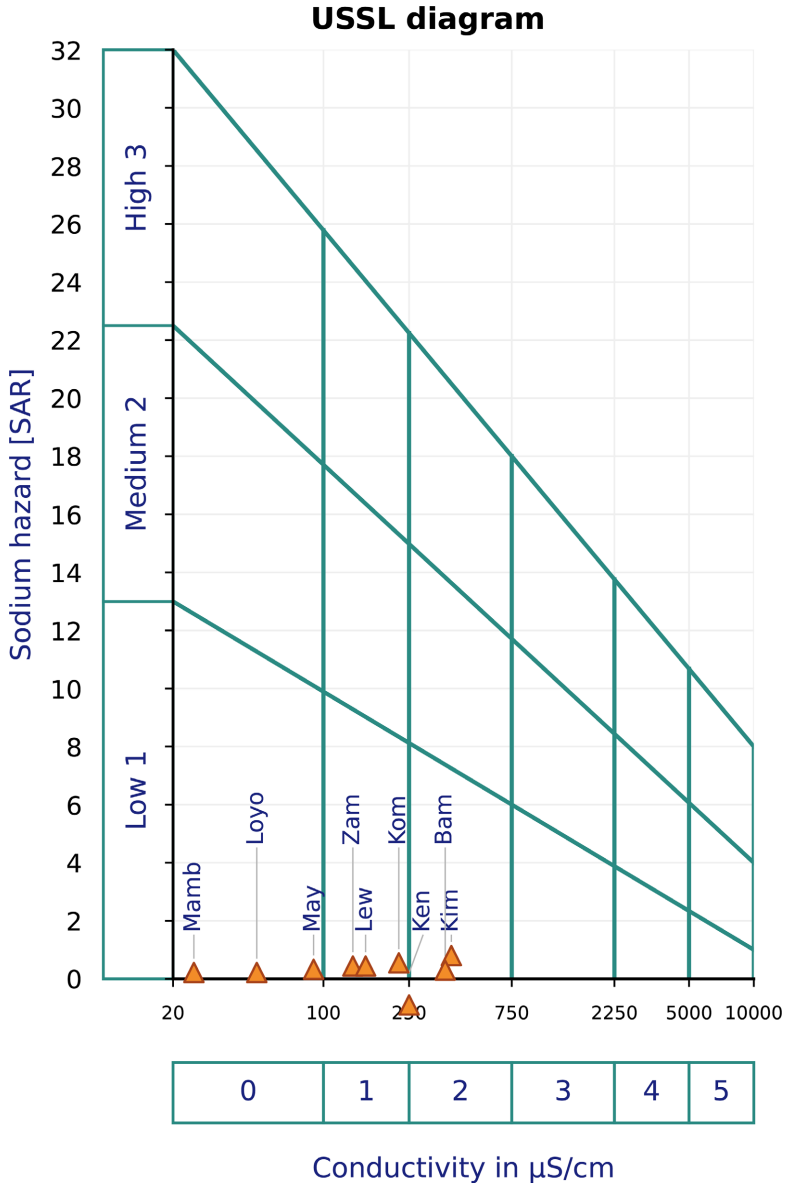


Figure 12. USSL diagram of the water.

These temperatures, close to that of the ambient air, are characteristic of the climate of the forest zone of the Lékoumou. They are close to those recorded in the Oyo area by [44] in the dry season. These low temperature values indicate the openness of the aquifer system [45], which generally makes the aquifer very vulnerable when it is located in areas of intensive land use. This water tends towards low acidity to neutrality, as its pH varies between 6.75 and 7.32. These values, which fall within the WHO acceptable range (6.5 - 8.5), are consistent with those reported by [44], [45] and [46]. However, the acidity of the water studied by these authors is higher than that of the water of our study area; this difference in acidity is due to the nature of the geological formations and the types of soil that the water passes through during recharge. The slightly acidic values observed at some water points of the aquifer studied could be due to the influence of CO_2 during recharge

by meteoric water. According to [47], in granitic formations, the input of CO_2 can lead to a decrease in the pH of groundwater and promote water-rock interactions. pH values close to neutrality suggest a moderate influence of CO_2 or a progressive neutralization of the acidity during underground circulation.

b) Electrical conductivity (EC) and TDS

Electrical conductivity (EC) and total dissolved solids (TDS) show low mean values, EC (55.36 µS/cm) and TDS (70 mg/L) (**Figure 3**), well within the WHO acceptable range (EC < 1000 µS/cm; TDS < 600 mg/L). The two parameters are strongly correlated (R = 0.93) (**Table 3**), which confirms their close relationship with the ionic load and the degree of mineralization of the water. The low values of electrical conductivity and total dissolved solids (TDS) observed in the groundwater reflect a low mineralization of the aquifer. This low mineralization could be explained by a relatively short residence time of the groundwater, thus limiting the action of the water on the soluble minerals of the aquifer formations and their accumulation. According to [48], an increase in the concentration of dissolved ions generally leads to a simultaneous increase in TDS and electrical conductivity (EC); conversely, a decrease in ion concentrations, through the absence of mineral dissolution, would lead to a decrease in TDS and EC values. The work carried out by [49] in the city of Brazzaville, by [45] in the shallow aquifers of Pointe-Noire, by [46] in the northern part of Brazzaville and by [44] in the northern part of the country highlights trends in electrical conductivity (EC) and total dissolved solids (TDS) similar to those observed in the present study. These results attest to a generally low mineralization of the shallow aquifers studied in the Congo.

2) Physicochemical parameters measured in the laboratory

a) Major cations: Ca^{2+}, Mg^{2+}, K^{+} and Na^{+}

The cations show low mean concentrations, Ca^{2+} (21.23 mg/L), Mg^{2+} (4.07 mg/L), Na^{+} (2.9 mg/L) and K^{+} (2.04 mg/L). These trends of low mean values were observed by [45] working on the water of the shallow coastal aquifer of Pointe-Noire. The means were as follows: Ca^{2+} (37.88 mg/L), Mg^{2+} (10.07 mg/L), Na^{+} (4.00 mg/L) and K^{+} (0.39 mg/L), although they were working in a coastal aquifer linked to the clayey-sandy formations and sandstones of the Cretaceous. They attribute the presence of these ions to the phenomenon of rain leaching of the soils and to anthropogenic activity. The Lékoumou area consists of calcareous sandstones, marly argillites, feldspathic sandstones, calc-alkaline granites and endomorphic granodiorite. The lithological diversity of these formations thus offers several potential sources of major cations, notably the dissolution of carbonate phases, the weathering of feldspars and cation exchange with clay minerals. As [50] point out, the concentrations of the main ions in groundwater are largely explained by mixing and water-rock interaction. The Ca^{2+} and Mg^{2+} ions of the sampled water would come respectively from the dissolution of the carbonate fraction of the calcareous sandstones and of the marly level for calcium (Ca^{2+}), or from the weathering of the calcic feldspars present in the feldspathic sandstone formations and granitoid rocks. The weathering of the ferromagnesian minerals

presents in the granitoid and granodioritic fractions, and/or exchanges between the water and the clay phases of the marly argillites, may be the main sources of enrichment of the water in Mg^{2+} ions.

Na^+ and K^+ ions may come mainly from the weathering of the feldspathic minerals present in the feldspathic sandstones, the calc-alkaline granites and the granodiorites.

b) The anions HCO_3^-, Cl^-, SO_4^{2-}

The major anions recorded in the sampled water have low mean values, which are respectively 83.15 mg/L, 7.16 mg/L and 22.17 mg/L. Some authors who have worked on groundwater in the Congo obtained values somewhat similar to ours, notably [45] (HCO_3^- = 100 mg/L, Cl^- = 6.38 mg/L and SO_4^{2-} = 5.07 mg/L) in the coastal region of Pointe-Noire and [44] (HCO_3^- = 83.15 mg/L and Cl^- = 18 mg/L). In the coastal region, the authors attribute the presence of the HCO_3^-, Cl^- and SO_4^{2-} ions to a single geochemical process, the weathering of the silicate minerals of the bedrock, the sands of the Cretaceous. In our context, the presence of different types of geological formations gives a different result. Bicarbonates (HCO_3^-) are an important indicator of water-rock interactions and can also come from the weathering of silicates under the influence of dissolved CO_2. The dissolution of the carbonate phases of the calcareous sandstones and marly argillites can release HCO_3^- ions, while the weathering of the silicates of the granitic and granodioritic rocks contributes to the enrichment of this groundwater. [51] show that the dissolution of carbonate rocks and the weathering of silicate rocks contribute strongly to the enrichment of water in bicarbonates. Sulfates (SO_4^{2-}) may come from the dissolution of sulfate minerals, the oxidation of sulfide minerals or atmospheric inputs owing to the openness of the aquifer system. The absence of nitrates in the sampled water makes it possible to attribute the origin of the chlorides to atmospheric inputs or to the dissolution of halite.

c) Hydrochemical facies and evolution of the composition of the water

Classification of the water by the Piper and Schoeller-Berkaloff diagrams

The results obtained from the Piper diagram highlight a clear dominance of water of the calcium-magnesium bicarbonate facies. These facies represent 99% of all the samples analyzed (**Figure 5**), reflecting a relative homogeneity of the hydrochemical composition of the groundwater studied. The Schoeller-Berkaloff diagram nicely complements this analysis by showing hydrochemical profiles with a broadly similar evolution among the different samples. These water profiles are characterized by a predominance of bicarbonate ions (HCO_3^-) among the anions and of calcium (Ca^{2+}) and magnesium (Mg^{2+}) ions among the cations (**Figure 6**).

The joint predominance of the HCO_3^-, Ca^{2+} and Mg^{2+} ions thus confirms the dominance of the calcium-magnesium bicarbonate facies in the groundwater of the study area. Several authors in different regions of the Congo have also highlighted this hydrochemical signature: [52], in the groundwater of the contact zone between the coastal sedimentary basin and the Lower Precambrian basement in the southwest of the Republic of the Congo, as well as [53], in the water of the

coastal aquifer of Pointe-Noire.

According to these authors, the presence of the calcium-magnesium bicarbonate facies would be mainly favored by the contribution of the weathering of the silicate minerals present in the sandy and granitic formations, through the interactions between the water and the sandy and granitic geological formations it crosses. In the present study, the predominance of the Ca-Mg- HCO_3^- facies also appears consistent with the hypothesis of a significant contribution from silicate mineral weathering processes. It could also be associated with a contribution from the dissolution of carbonate phases present in some formations of the study area.

These combined results from the Piper and Schoeller-Berkaloff diagrams provide a first argument in favor of an origin mainly related to water-rock interactions, with a probable contribution from the weathering of silicates and possibly from the dissolution of carbonate phases.

d) Principal component analysis (PCA) and agglomerative hierarchical clustering (AHC)

The main associations between the physicochemical parameters, as well as the groupings of samples with similar hydrochemical characteristics highlighted by principal component analysis (PCA) and agglomerative hierarchical clustering (AHC), make it possible to complete the hydrochemical interpretation of the groundwater. Comparing the results of these two multivariate methods helps to better identify the geochemical processes likely to control the mineralization of the water and to specify the factors responsible for its spatial variability [54].

The results of the principal component analysis (PCA) show strong positive correlations of the variables Ca^{2+}, Mg^{2+}, HCO_3^- and electrical conductivity (EC) with the first factorial axis (F1). This association reflects a common contribution of these variables to the structuring of the hydrochemical variability of the groundwater, and suggests the existence of a mineralization gradient. This gradient could be mainly related to water-rock interactions, notably the dissolution of carbonate phases, as well as the weathering of the silicate minerals present in the geological formations of the study area.

The agglomerative hierarchical clustering (AHC) mainly distinguishes two associations: Ca^{2+} and Mg^{2+} grouped in the same class, while HCO_3^- and EC form another class. The grouping of the Ca^{2+} and Mg^{2+} cations reflects a relatively similar geochemical evolution of these two cations, likely resulting from their mobilization by common geochemical processes, notably the weathering and dissolution of the minerals of the formations making up the aquifer. This interpretation is supported by the dominance of the calcium-magnesium bicarbonate facies highlighted by the Piper diagram, which testifies to the importance of Ca-Mg-HCO_3 in the composition of the water studied. Comparable observations were reported by [49] in the groundwater of southwestern Congo, where a dominance of the Ca-Mg-HCO_3 facies was highlighted in the AQ-2 aquifer of Pointe-Noire.

The grouping of HCO_3^- and EC in the same class may, for its part, reflect a

concomitant evolution of these two parameters and the importance of bicarbonates in the overall mineralization of the water. Indeed, EC is an integrating indicator of the concentration of dissolved ionic species. Its proximity to the bicarbonate ions in the AHC thus suggests that variations in the HCO_3^- concentration contribute significantly to variations in the degree of mineralization of the groundwater. However, this association does not mean that bicarbonates alone are the cause of the conductivity, which is also controlled by all the dissolved ions present in the water.

e) Origins of the major ions and mineralization processes

The ionic relationships are highlighted through the bivariate diagrams (**Figure 10**), which make it possible to examine the correlations between different ions and, thus, to better understand their origin and the geochemical processes that control their distribution in the groundwater. In addition, the Gibbs diagram makes it possible to identify the geochemical mechanism likely to control the mineralization of the water, notably water-rock interactions, precipitation and evaporation processes, and inputs from precipitation.

f) Relationships between major ion ratios

The ionic relationships highlight strong correlations between the dissolved ions.

The Na^+ versus Cl^- plot shows a strong correlation ($R^2 = 0.76$), but all the samples lie above the equivalence line (1:1). Thus, since Na^+ concentrations exceed those of Cl^-, this indicates a release of Na^+ by the weathering of sodic silicates during water-rock interaction (Aghazadeh et al., 2017) or the influence of ion exchange [55]. These observations are consistent with the lithological nature of the study area, characterized by the presence of feldspathic sandstones and granitoid formations.

The relationship between $Ca^{2+} + Mg^{2+}$ and HCO_3^- shows an almost perfect correlation ($R^2 = 0.99$), but with an excess of $Ca^{2+} + Mg^{2+}$ relative to the 1:1 line. This observation clearly indicates that these cations are not exclusively associated with bicarbonates and that a fraction of their charge could be balanced by other ions, such as sulfates. The relationship between $(Ca^{2+} + Mg^{2+})$ versus $(SO_4^{2-} + HCO_3^-)$, with a strong correlation ($R^2 = 0.97$), corroborates this hypothesis, since all the samples lie below the 1:1 line. The results of these bivariate plots as a whole thus suggest a combined contribution of bicarbonates and sulfates to the balancing of the Ca^{2+} and Mg^{2+} cations.

These results are consistent with those of the Piper diagram, which highlights a dominance of the calcium-magnesium bicarbonate facies. They suggest that the mineralization of the groundwater results mainly from interactions between the water and the aquifer formations, with a contribution from the dissolution of carbonate phases and the weathering of silicate minerals. However, the deviations observed from the 1:1 line in the different bivariate diagrams suggest that several geochemical processes act concomitantly in shaping the chemical composition of the groundwater studied.

g) Gibbs diagram

The Gibbs diagram shows a clear predominance of samples in the water-rock interaction domain. This distribution suggests that exchanges between infiltrating water and the geological formations of the aquifer are the main mechanism controlling the mineralization of the groundwater of the Lékoumou. According to [56], the chemical composition of natural waters is mainly controlled by three major geochemical mechanisms: water-rock interactions, meteoric inputs and evaporation-crystallization processes. However, it should be noted that the interpretation of the Gibbs diagram must be treated with caution, because in the case of groundwater the composition may also result from the simultaneous action of several processes, notably mineral dissolution and weathering, ion exchange, water mixing, residence time and underground circulation conditions [50].

In the study area, the presence of calcareous sandstones, marly argillites, feldspathic sandstones, calc-alkaline granites and endomorphic granodiorites constitutes a geological context favorable to the dissolution and release of the different chemical elements into the groundwater. The presence, notably, of Ca^{2+}, Mg^{2+} and HCO_3^- can thus be associated with the weathering and dissolution processes of the minerals making up these geological formations during the infiltration and underground circulation of the water. The predominance of the water-rock interaction domain in the Gibbs diagram, together with the analyses of ionic relationships highlighted in the bivariate diagrams and the multivariate analyses, thus makes it possible to retain water-rock interaction as the main geochemical mechanism controlling the mineralization of the groundwater of the Lékoumou. This mechanism would be mainly favored by the infiltration and circulation of meteoric water through the crystalline basement and the sedimentary formations, during which weathering, dissolution and ion exchange processes contribute to the acquisition of the mineral load of the water.

h) Suitability of the groundwater for irrigation

The suitability of the water of the Lékoumou for irrigation was assessed on the basis of the sodium percentage (%Na), the sodium adsorption ratio (SAR), the magnesium adsorption ratio (MAR), the permeability index (PI), as well as the Wilcox and USSL diagrams. Comparing the results of these different indicators makes it possible to appraise in an integrated manner the risks associated with salinity, sodicity and the alteration of the physical properties of soils. This approach thus makes it possible to characterize water quality for agricultural use and to identify possible constraints related to its use for irrigation.

The results for the sodium percentage (%Na) and the sodium adsorption ratio (SAR) indicate, according to the classification of [38], that the groundwater sampled in the Lékoumou falls in the excellent to good categories. Furthermore, all the samples are positioned in class S1 of the USSL diagram, corresponding to a low sodicity hazard. These results indicate that the groundwater studied is favorably suited to irrigation. These results are consistent with those obtained by [57] in the water of the AQ-2 aquifer of the Pointe-Noire area, which also showed good

suitability of the water for agricultural use [58].

The magnesium adsorption ratio (MAR) values obtained for all the water samples are below 50%. According to the threshold proposed by [39], these values indicate that the groundwater sampled in the Lékoumou is suitable for irrigation and does not present a significant risk related to a high proportion of magnesium likely to affect the physical properties of soils. Moreover, the permeability index (PI) shows that 30% of the samples belong to class I and 70% to class II. According to the classification of [43], these two classes correspond to water that can be used for irrigation. These results thus suggest that the use of this water should not lead, under the conditions studied, to significant soil degradation.

The Wilcox and USSL diagrams, based respectively on the relationship between %Na and electrical conductivity (EC), and between SAR and electrical conductivity (EC), broadly confirm the results obtained from the different indicators. The groundwater sampled in the Lékoumou falls in the good category of the Wilcox diagram and in classes C1S1 and C2S1 of the USSL diagram. The latter correspond respectively to a low to moderate salinity hazard and to a low sodicity hazard. This trend is comparable to that reported by [44] for the groundwater of the Alima basin.

Overall, the convergence of the results obtained from %Na, SAR, MAR, PI and the Wilcox and USSL diagrams shows that the groundwater sampled in the Lékoumou is, on the whole, well suited to irrigation. Its agricultural use thus appears unlikely to give rise, under current conditions, to major problems of salinity, sodicity or degradation of soil permeability.

5. Conclusions

This study focused on the assessment of the hydrochemical characteristics of the groundwater of the Lékoumou, with the objective of appraising its quality with regard to the requirements for water intended for human consumption and of assessing its suitability for irrigation. All the results obtained show that the groundwater studied has an overall satisfactory physicochemical quality. The [22] does not set health-based limit values for most of the analyzed parameters; however, the measured concentrations remain below the existing acceptability thresholds. The pH values, characterized by low acidity to near-neutrality, also indicate that this water does not present a major risk of aggressiveness towards drainage structures.

From the hydrochemical standpoint, the groundwater sampled in the Lékoumou is very largely characterized by a calcium-magnesium bicarbonate facies. The dominant ions are bicarbonates (HCO_3^-), calcium (Ca^{2+}) and magnesium (Mg^{2+}). The analysis of ionic relationships, coupled with the hydrochemical diagrams and the statistical treatments, suggests that the mineralization of the water is mainly controlled by water-rock interactions, notably by mineral dissolution and weathering processes, to which ion exchange phenomena may be added.

The assessment of the suitability of the water for irrigation, based on the values

of the sodium percentage (%Na), the sodium adsorption ratio (SAR), the magnesium adsorption ratio (MAR) and the permeability index (PI), as well as on the Wilcox and USSL diagrams, indicates that this water is, overall, well suited to agricultural use. Its use should therefore not give rise, under the conditions studied, to significant risks related to salinity, sodicity or the degradation of the physical properties of soils.

Thus, the groundwater sampled in the Lékoumou globally presents physicochemical characteristics that are favorable both for human consumption and for irrigation. However, although the physicochemical parameters analyzed do not exceed the WHO acceptability thresholds, regular and rigorous monitoring of the quality of this water, including in particular biological analyses as well as analyses carried out in both the wet and dry seasons, remains necessary to ensure sustainable management of the resource, guarantee its potability and preserve the health of the population.

Author Contributions

Gilbert BASSAKOUAHOU, fieldwork and sampling, conceptualization, methology and data analysis. Hartman Issombo Elenga, methodology and data analysis, Djohn Josia Weaver MBOUSSA, data analysis, MPIKA NGOUAKA Lydie Natacha, fieldword and laboratory analysis. Urbain Gampio Mbilou and Medar NGOUALA MAMBOZO, supervision. All authors have read and agreed to the published version of the manuscript.

Conflicts of Interest

The authors declare no conflicts of interest regarding the publication of this paper.

References

[1] UNICEF (2024) UNICEF Annual Report 2024. 56 p. https://www.unicef.org/reports/unicef-annual-report/2024

[2] Tampo, L., Ayah, M., Kodom, T., Tchakakla, I., Boguido, P., Bawa, L., *et al.* (2014) Impact De La Demande En Chlore Et De La Chloration Sur La Désinfection Des Eaux De Puits Des Quartiers De Lomé: Cas Des Quartiers De Démakpoé Et D'agbalépédogan (togo). *Journal of Applied Biosciences*, **75**, 6272. https://doi.org/10.4314/jab.v75i1.12

[3] WHO, UNICEF (2019) 1 in 3 People Globally Do Not Have Access to Safe Drinking Water. Press Release (New York/Geneva). https://www.who.int/news/item/18-06-2019-1-in-3-people-globally-do-not-have-access-to-safe-drinking-water-unicef-who

[4] UNICEF (2025) Water, Sanitation and Hygiene: For Every Child. UNICEF Congo. https://www.unicef.org/congo/eau-hygi%C3%A8ne-et-assainissement

[5] Queneau, P., Hubert, J., Bourre, J.M., Couturier, D., Duhamel, J.F., Menkès, C.J., *et al.* (2006) Place des eaux minérales dans l'alikmentation. *Bulletin de l'Académie Nationale de Médecine*, **190**, 2013-2021. https://doi.org/10.1016/s0001-4079(19)33143-7

[6] Duhamel, J.F. and Brouard, J. (2010) L'eau et l'hydratation: une nécessité pour la vie.

Journal de Pédiatrie et de Puériculture, **23**, 9-12.
https://doi.org/10.1016/j.jpp.2009.12.002

[7] Journal Officiel de la République du Congo (Official Gazette of the Republic of the Congo). 55th Year, No. 23, 2013. https://www.sgg.cg/JO/2013/congo-jo-2013-23.pdf

[8] Ofouémé-Berton, Y. (2010) L'approvisionnement en eaux des population rurales au Congo-Brazzaville. *Cahiers d'Outre-Mer*, **63**, 7-30. https://doi.org/10.4000/com.5838

[9] Tribune Eco (2025) Approvisionnement en eau.

[10] Yao, T., Oga, M., Fouche, O., Baka, D., Pernelle, C. and Biemi, J. (2013) Evaluation de la potabilité chimique des eaux souterraines dans un bassin versant trpoical: Cas du sud-ouest de la Côte d'Ivoire. *International Journal of Biological and Chemical Sciences*, **6**, 7069-7086. https://doi.org/10.4314/ijbcs.v6i6.42

[11] UNICEF (2019) Eau, Hygiene et Assainissement. Pour chaque enfant un accès equitable et durable à l'eau et à l' assainissement.
https://www.unicef.org/congo/eau-hygiène-et-assainissement

[12] Miassouka, Milandou, F., Moulada, Nimy, E.N. and Ngoka V. (2023) Caractérisation physico-chimiques des eaux desurface et souterraines du district de Bambama (Département de la Lékoumou): Origine de la minéralisation et potabilité des eaux. *Géologie et ressources naturelles en Afrique Centrale*: *Impact sociétal et développement durable*, *livre des résumés*, Brazzaville, 5-7 December 2023, 74.

[13] Samba-Kimbata, M.J. (1978) Le climat du bas-Congo. Ph.D. Thesis (3rd Cycle), Université de Bourgogne, 280 p.

[14] De Bouassezon, P. and Gras, F. (1970) Notice explicative n˚ 44. Carte pédologique Sibiti-est. Rép. du Congo B/ville 1/500000.
https://www.documentation.ird.fr/hor/fdi:04607

[15] Novikoff, A. (1967) Altération des roches dans le massif du Chaillu (R. Congo). Cahier n˚1-Géologie de la Région. Document ORSTOM: MC 149, 39 p.

[16] Novikoff, A. (1974) Altération des roches dans le massif du chaillu. Ph.D. Thesis, Université Louis Pasteur, 316 p.

[17] Sofreco-Cerape (2011) Etude du secteur Agricole-République du Congo: Monographie départementale de la Lékoumou. Brazzaville, Républiqude. du Congo.
https://fr.scribd.com/document/598892314

[18] Boundzanga, G.C. (2014) Rapport d'étude sur la consommation du bois-énergie en Rép. du Congo CN-REDD. 101 p.
https://wri-sites.s3.amazonaws.com/forest-atlas.org/cog.forest-atlas.org/resources/docs/Re

[19] Novikoff, A. (1967) Alteration des roches dans le massif du chaillu (R. Congo) Cahier N˚ 1-Géologie de la Région. Doc ORSOM: MC 149, 39 p.

[20] Denis, B. and Bosseno, R. (1977) Généralité Mayoko-Komono. ORSTOM n˚200, Vol. I, 649 p.

[21] Samba, J.L. and Saya, R.A. (2012) Deuxième rapport national sur les ressources génétiques forestières de la République du Congo. Coordination nationale de SAFORGEN, République du Congo. https://www.fao.org/4/i3825e/i3825e14.pdf?utm

[22] WHO (2017) Guidelines for drinking-Water Quality. 4th Edition, Incorporating the First Addendum.

[23] OMS (2024) Directives pour la qualité de l'eau de boisson: Quatrième édition intégrant le premier addendum. Organisation mondiale de la Santé.

[24] Anongba Braphond, R.V.B., Privat, T., Issa, S.S. and Germain, A.M. (2023) Origine

et processus de minéralisation des eaux souterraines dans la partie sud du Marais Poitevin (Nouvelle-Aquitaine, France) et de son substratum carbonaté de l'Oxfordien supérieur. *European Scientific Journal, ESJ*, **19**, 231-261. https://doi.org/10.19044/esj.2023.v19n33p231

[25] BRGM (2016) Mise en place d'un réseau de suivi de la qualité des eaux souterraines sur les bassins versants de Horn et du Guillec-Etape 3: Interprétation des résultats d'analyses 2015. Progress report BRGM/RP-65567-FR, 46 p.

[26] Diabagaté, A., Goula, T.A. and Soro, G.E. (2019) Hydrochimie des eaux souterraines de la région du poro (Côte d'Ivoire). *European Scientific Journal, ESJ*, **15**, 247-262. https://doi.org/10.19044/esj.2019.v15n9p247

[27] Elsayed, S., Hussein, H., Moghanm, F.S., Khedher, K.M., Eid, E.M. and Gad, M. (2020) Application of Irrigation Water Quality Indices and Multivariate Statistical Techniques for Surface Water Quality Assessments in the Northern Nile Delta, Egypt. *Water*, **12**, Article No. 3300. https://doi.org/10.3390/w12123300

[28] Youssef, Y.A., Abuarab, M.E., Mahrous, A., Farag, E., Yan-Li, L., Wen-Hui, Y., *et al.* (2026) Hydrochemical and GIS-Based Evaluation of Groundwater Suitability for Irrigation Using IWQI in the Desert Hinterland of Western Nile Delta Egypt. *Scientific Reports*, **16**, Article No. 8724. https://doi.org/10.1038/s41598-026-39089-z

[29] Chaweye, Y.N., Ousmane, B.I., Nazoumou, Y., Favreau, G., Boucher, M. and Mahaman, R.A. (2025) PProcessus de minéralisation et impact de l'irrigation sur les ressources en eau souterraine au Sahel: Cas du périmètre irrigué de Birni N'Konni (Sud-Niger). *European Scientific Journal, ESJ*, **21**, 175-200. https://doi.org/10.19044/esj.2025.v21n24p175

[30] Orou, R.K., Soro, G., Soro, D.T., Fossou, R.M.N., Onetie, O.Z., Ahoussi, E.K., *et al.* (2016) Variation Saisonnière De La Qualité Physico-Chimique Des Eaux Souterraines Des Aquifères d'Altérites Du Département d'Agboville (Sud-Est De La Côte d'Ivoire). *European Scientific Journal, ESJ*, **12**, 213-240. https://doi.org/10.19044/esj.2016.v12n17p213

[31] Abboudi, A., Tabyaoui, H., El Hamichi, F., Benaabidate, L. and Lahrach, A. (2014) Etude de la qualité physicochimique et contamination métallique des eaux de surface du bassin versant de Guigou, Maroc. *European Scientific Journal*, **10**, 83-96. https://eujournal.org/index.php/esj/article/download/3936/3728/0

[32] Atekwana, E., Atekwana, E., Rowe, R., Werkemajr, D. and Legall, F. (2004) The Relationship of Total Dissolved Solids Measurements to Bulk Electrical Conductivity in an Aquifer Contaminated with Hydrocarbon. *Journal of Applied Geophysics*, **56**, 281-294. https://doi.org/10.1016/s0926-9851(04)00057-6

[33] Steli, S., Hilali, M., Mahboub, A., Rachid, L. and Barbot, A. (2019) Groundwater Quality Assessment of the Jrf-Ferzna Palm Grove (South-Eastern Morocco). *Environmental and water Sciences, Public Health and Territorial Intelligence Journal*, **3**, 231-237.

[34] Cano-Paoli, K., Chiogna, G. and Bellin, A. (2019) Convenient Use of Electrical Conductivity Measurements to Investigate Hydrological Processes in Alpine Headwaters. *Science of the Total Environment*, **685**, 37-49. https://doi.org/10.1016/j.scitotenv.2019.05.166

[35] Li, H., Noir, J.R., Hao, Y., Hao, P., Mishra, U.N. and Haese, R.R. (2024) Modélisation des réactions diagénétiques et de la génération de porosité secondaire dans les grès, contrôlées par l'advection d'acides organiques de faible masse moléculaire. *Basin Research*, **36**, e12860.

[36] Mussa, C.J. and Kamoto, J.F.M. (2023) Évaluation de la qualité des eaux souterraines

dans les zones urbaines du Malawi: Le cas de la zone 25 à Lilongwe. *Journal of Environmental and Public Health*, **2023**, Article ID: 6974966.

[37] Arveti, N. (2025) Hydrogeochemical Characteristics and Evaluation of Groundwater Quality in Varadaiahpalem, Andhra Pradesh, South India. *Discover Environment*, **3**, Article No. 264. https://doi.org/10.1007/s44274-025-00447-9

[38] Wilcox, L.V. (1955) Classification and Used of Irrigation Water. U.S. Department of Agriculture, Circular No. 969, 19 p.

[39] Hussein, H., El Maghraby, M.M.M. and Abu Salem, H.S. (2024) Application de l'indice de qualité de l'eau et des techniques statistiques-hydrochimiques à l'évaluation des eaux souterraines de l'aquifère quaternaire du delta du Nil sud-ouest en Égypte. *Applied Water Science*, **14**, 143.

[40] Anim-Gyampo, M., Anornu, G.K., Appiah-Adjei, E.K. and Agodzo, S.K. (2019) Quality and Health Risk Assessment of Shallow Groundwater Aquifers within the Atankwidi Basin of Ghana. *Groundwater for Sustainable Development*, **9**, Article ID: 100217. https://doi.org/10.1016/j.gsd.2019.100217

[41] Raghunath, H.M. (1987) Groundwater. 2nd Edition, Wiley Eastern Limited, 344-369.

[42] Gonzalez-Acevedo, Z.I., Paddilla-Rdeyes, D.A. and Rmos-Leal, J.A. (2016) Quality Assessment of Irrigation Water Related to Soil Salinization in Tierra Nueva, San Luis Potosi, Mexico. *Revisita Mexicana de Ciencias Geologicas*, **33**, 271-285.

[43] Doneen, L.D. (1964) Notes on Water Quality in Agriculture, Part 1. Water Science and Engineering Paper No. 4001, Department of Water Science and Engineering, University of California.

[44] Mouakoumbat, N.J.L., Ebotehouna, C.G. and Mbilou, U.G. (2025) Suivi des Paramètres Physico-Chimiques des Eaux Souterraines du Bassin de l'Alima, affluent du Fleuve Congo: Campagnes de Grande Saison Sèche 2021 et 2022 dans les Districts d'Oyo, Tchikapika et Boundji, République du Congo. *European Scientific Journal, ESJ*, **21**, 96-121. https://doi.org/10.19044/esj.2025.v21n18p96

[45] Mbilou, U.G., Tchoumou, M., Ngouala, M.M. and Balounguidi, J. (2016) Caracterisation hydrogeochimique et microbiologique des eaux souterraines dans le systeme d'aquiferes multi couche de la region de pointe-noire en republique du congo. *Larhyss Journal*, No. 28, 257-273. http://creativecommons.org/licenses/by/4.0

[46] Essouli, O.L. (2024) Hydrochimie, qualite physico-chimique et bacteriologique des eaux de la partie nord de brazzaville (republique du congo). *International Journal of Recent Scientific Research*, **15**, 5048-5059. http://www.recentscientificcom

[47] Kim, K., Jeong, D.H., Kim, Y., Koh, Y.K., Kim, S.H. and Park, E. (2008) The Geochemical Evolution of Very Dilute CO_2-Rich Water in Chungcheong Province, Korea: Processes and Pathways. *Geofluids*, **8**, 3-15. https://doi.org/10.1111/j.1468-8123.2007.00200.x

[48] Rusydi, A.F. (2018) Correlation between Conductivity and Total Dissolved Solid in Various Type of Water: A Review. *IOP Conference Series: Earth and Environmental Science*, **118**, Article ID: 012019. https://doi.org/10.1088/1755-1315/118/1/012019

[49] Marandi, A. and Shand, P. (2018) Groundwater Chemistry and the Gibbs Diagram. *Applied Geochemistry*, **97**, 209-212.

[50] Gaillardet, J., Dupré, B. and Allègre, C.J. (1995) A Global Geochemical Mass Budget Applied to the Congo Basin Rivers: Erosion Rates and Continental Crust Composition. *Geochimica et Cosmochimica Acta*, **59**, 3469-3485. https://doi.org/10.1016/0016-7037(95)00230-w

[51] Ngouala Mabonzo, M. (2020) Caractérisation hydrochimique des eaux souterraines

de la zone de contact du bassin sédimentaire côtier et du socle du Précambrien inférieur au sud-ouest de la République du Congo. *Cinq Continents*, **10**, 60-85.

[52] Nkounkou Tomodiatounga, D., Mabiala, B. and Moukandi Nkaya, G. (2016) Hydrochemical Characteristics of the Groundwater AQ1 of the Region from Pointe-Noire to Congo Brazzaville. *Journal of Geoscience and Environment Protection*, **4**, 95-109. https://doi.org/10.4236/gep.2016.49008

[53] Cloutier, V., Lefebvre, R., Therrien, R. and Savard, M.M. (2008) Multivariate Statistical Analysis of Geochemical Data as Indicative of the Hydrogeochemical Evolution of Groundwater in a Sedimentary Rock Aquifer System. *Journal of Hydrology*, **353**, 294-313. https://doi.org/10.1016/j.jhydrol.2008.02.015

[54] Matini, L., Moutou, J.M. and Kongo-Mantono, M.S. (2010) Evaluation Hydro-Chimique Des Eaux Souterraines En Milieu Urbain Au Sud-Ouest De Brazzaville, Congo. *Afrique Science*: *Revue Internationale des Sciences et Technologie*, **5**, 82-98. https://doi.org/10.4314/afsci.v5i1.61709

[55] Aghazadeh, N. and Mogaddam, A.A. (2011) Investigation of Hydrochemical Characteristics of Groundwater in the Harzandat Aquifer, Northwest of Iran. *Environmental Monitoring and Assessment*, **176**, 183-195. https://doi.org/10.1007/s10661-010-1575-4

[56] Aweda, A.K., Jatau, B.S. and Goki, N.G. (2023) Groundwater Geochemistry and Hydrochemical Processes in the Egbako Aquifer, Northern Bida Basin, Nigeria. *Revista Brazileira de Recursos Hidricos*, **28**, e31. https://doi.org/10.1590/2318-0331.282320230010

[57] Gibbs, R.J. (1970) Mechanisms Controlling World Water Chemistry. *Science*, **170**, 1088-1090. https://doi.org/10.1126/science.170.3962.1088

[58] Tathy, C., Matini, L., Moukandi, Nkaya, G. and Mabiala, B. (2011) Assessing Factors Controlling the Hydrochemistry and Suitability for Irrigation Purposes of Aquifer AQ-2 in Point-Noire, South-West Congo-Brazzaville. *Research Journal of Applied Sciences*, *Engineering and Technology*, **3**, 617-624. https://maxwellsci.com/print/rjaset/v3-617-624.pdf